BIO Web of Conferences **116**, 06011 (2024) https://doi.org/10.1051/bioconf/202411606011
EBWFF 2024

Modeling of light transmission in multilayer epitaxial AlN/GaN structures for biomedical pyrosensors

Eugeny Panyutin[1*] and *Tatiana* Ilicheva[2]

[1]Ioffe Institute, 194021, Polytechnicheskaya 26, St-Petersburg, Russia
[2]Admiral Makarov State University of Maritime and Inland Shipping, 198035, St-Petersburg, Russia

Abstract. The spectral-pulse diversity of modern lasers currently used for subcutaneous surgeries provides ample opportunities for the realization of rather complex modes of radiation exposure and allows the simultaneous performance of diagnostic, therapeutic and surgical procedures; this in turn leads to an urgent need for appropriate spectrally indifferent sensors oriented for in vivo operation. In the present work, we propose the use of weakly absorbing epitaxial GaN/AlN/GaN structures as a basis for the fabrication of pass-through pyrometric sensors embedded in a subcutaneous light guide. The use of such sensors in vivo will allow the local study of the absorption or scattering of intracavitary tissues in a wide spectral range, as well as the real-time control of the pulse structure of the laser beam. For such structures, a mathematical model of light propagation taking into account absorption and heat generation was constructed and a computational algorithm for obtaining post-pulse temperature distributions and for calculating the pyrocoefficient at different values of thickness and donor concentration of absorbing GaN layers was developed in the MATLAB environment. A criterion for the efficiency of the sensor performance was proposed, based on which the optimal ratios between the thickness values of AlN and GaN layers for different values of the absorption coefficient α_{GaN} were obtained. Key words: subcutaneous operations, laser therapy, laser surgery, pyroeffect, pyrosensors, aluminum nitride, epitaxial technologies, multilayer GaN/AlN structures.

1 Introduction

Sensors based on the pyroelectric effect have long been used for diagnostics and measurement of energy parameters of pulsed laser radiation [1, 2], but due to the emergence of new applications of lasers, including for solving various medical problems [3, 4], there is an urgent need for the development of new diagnostic tools.

Nowadays lasers are successfully used for instance for myocardial revascularization in case of non-shuntability of coronary arteries to form artificial channels (single pulses of millisecond duration [5, 6]). Lasers are also used for cancer therapy (detection of tumor localization using luminescent photosensitizers and subsequent exposure to powerful

* Corresponding author: eugeny.panyutin@mail.ioffe.ru

destructive pulses) [7-9]. [7-9]. Lithotripsy operations are also known, providing defragmentation of unwanted solid formations using long series of non-periodic pulses, which leads to destruction of the target as a result of photoacoustic effect [10]. Traditional application of lasers in ophthalmology in the form of refractive microsurgery uses picosecond and femtosecond modes [11].

Thus, the use of laser exposure allows to provide diagnostic, therapeutic and surgical procedures, including those applied to the same intracavity object. This, in turn, may require the combination of several laser modes and the organization of a very complex spectral-pulse structure of radiation, which is achievable with the joint use of several different lasers.

On the other hand, the emerging tendency to complicate the temporal structure of the beam creates the need for control systems based on recording and measuring the energy parameters of laser impulses in real time and directly during the beam exposure. Such systems could be a useful addition to the visualization tools during the relevant subcutaneous operations, as well as provide the possibility of rapid response in cases of inadvertent deviation of beam parameters (for instance, pulse energy or pulse repetition rate) beyond the specified parameters.

Since a significant part of laser operations are of subcutaneous and laterascopic type, the integral elements of the optical path are the means of radiation delivery to the area of direct action (light guides), this objective can be solved by using pass-through optical sensors, almost transparent in the whole spectral range and embedded directly into the optical path. One of the possible approaches to its solution is the use of sensors based on the pyro-effect (appearance of electrical signals at temperature change), which is typical for crystals having a suitable type of crystal lattice and, in particular, AlN. The undoubted advantages of this material, among others, are chemical indifference and excellent biocompatibility, which allows its use directly in vivo and has already led to the appearance of piezosensor chips for continuous monitoring of blood pressure [12-14], so that the development of pyrosensor elements for instance for in vivo research of local absorption and scattering ratio, is also relevant.

The main purpose of this work is computer simulation and research of light transmission features in GaN/AlN/GaN epitaxial structures (in which electrically conducting GaN layers play the role of electrodes) and optimization of parameters of such structures from the point of view of obtaining maximum pyro-ot-click at a given level of transparency.

2 Materials and structure of the sensor

It is well known that the pyroelectric effect (change in the polarization of a crystal when its temperature changes and, in particular, when absorbing radiant energy) is characteristic of some types of crystals (namely, those having a lattice like wurtzite or perovskite) and manifests itself when heated in the form of the emergence of charge on its opposite faces. In the case of sufficiently low conductivity of the crystal, this excess charge is not compensated by free carriers, remains for a long time and can be easily registered.

Since the effect of a laser pulse leads to heating of the target, pyroelectric materials have long been used in laser radiometry to measure the energy of pulses, however, due to the absence or difficult availability of the corresponding single crystals, until recently, opaque polycrystalline composites (ceramics based on ZrPbTaO3, LiTaO3 or ZnO) were used for sensor elements.

At the same time, the intensive development of epitaxial technologies of semiconductor III-nitrides (GaN, AlN) and wide-gap oxides (Ga2O3, ZnO), observed in recent years and associated with the development of the UV range, has created prerequisites for obtaining

crystallographically perfect epitaxial layers on various substrates [15,16], studying their thermophysical properties [17], and stimulated the research of pyroelectric effect in epitaxial AlN-structures [18,19].

The basis for the choice of aluminum nitride as a material for the basic sensor element for bio-medical applications among other pyroelectric materials are the following considerations. Being a large bandgap semiconductor (width of the forbidden zone Eg=5.9eV), unalloyed AlN is transparent up to the UV region, has the lowest conductivity among known pyroelectrics, high mechanical strength, chemical resistance, and thermostability of parameters [20]. In addition, an important advantage of AlN in the considered perspective is its technological compatibility with other materials (GaN, Ga2O), allowing to obtain high quality multilayer structures.

Earlier [21], an epitaxial structure of an almost transparent GaN/AlN/GaN sensor with a transparent AlN layer and weakly absorbing GaN layers was proposed to register such high-intensity single laser pulses that low absorption was a necessary condition to prevent its destruction. Modeling of powerful light fluxes and significant heat generation in the absorbing layers allowed us to develop recommendations for the optimal thickness ratio and doping level in terms of reducing thermoelastic stresses arising at the sensor hetero-boundaries.

Such a three-layer structure of the electrode - sensing layer - electrode type is the simplest, therefore, taking into account the desirability of the sensor area limitations, the question of the practicality of complicating the structure, including by increasing the number of such three-layer functional groups of layers located along the path of the light beam. In this case, the possibility of parallel inclusion of these sensors creates additional opportunities to reduce the necessary absorption coefficient of αGaN, providing a given level of output signal. This reduction αGaN leads to a decrease in the maximum temperature, which is desirable from the point of view of reducing thermal stresses arising at hetero-boundaries is of undoubted interest. At the same time, a relatively simple case of doubling of such basic sensor groups of layers can be realized using double-sided epitaxy, which is the most acceptable from the point of view of technological realization (see [16]). It is assumed that when performing post-epitaxial operations, it is not difficult to create such interconnections that these sensor substructures would be electrically switched on in parallel. In such a scheme, the pyroelectric response will be determined by the total surface charge appearing on the surfaces of all AlN layers as they are heated by a passing light pulse.

In the present research, computer simulations of light fluxes and heat generation in absorbing layers in such double structures epitaxially produced on two sides of an Al_2O_3- or SiC-substrate have been carried out, with the focus on optimizing the parameters (thickness and doping level) of the layers to obtain the maximum sensor pyroresponse.

The proposed and investigated sensor structure is primarily oriented to HVPE-technology, within the framework of which it is possible to controllably obtain layers with the thickness of ~0.5÷200μm. AlN layers demonstrate the properties of a typical dielectric with record low conductivity, and semiconductor GaN layers during growth using SiO_2 reactor are characterized by background introduction of oxygen and silicon atoms creating small donor levels (n-type) with the concentration of N_d centers, allowing technological control in the range of $10^{18} \div 10^{20}$cm^{-3}.

Since the width of the forbidden zone E_g for GaN is 3.39 eV, the edge of the fundamental absorption corresponds to ~λ=0.33 μm, and at longer wavelength of radiation its absorption occurs mainly on free carriers (on electrons in the case of n-type semiconductor), which is expressed in particular in the proportionality of the light absorption coefficient α_n of donor concentrations N_d.

This important circumstance suggests that doped GaN layers at a certain ratio of their thickness and donor concentration N_d (considering that at ordinary temperatures the concentration of free electrons $n \approx N_d$) can be almost transparent, and due to the high mobility of electrons μ_n maintain acceptable conductivity values ρ.

This statement follows, among other things, from the fundamental formula for α_n (see [21] and the references cited).

$$\alpha_n = G_o \cdot (\lambda^2 n)/\mu_n \quad \text{or} \quad \alpha_n = G_o \cdot (\lambda^2 N_d)/\mu_n \tag{1}$$

where $$G_o = e^3/(4\pi^2 \varepsilon_0 \cdot c^3 m*_n \cdot n_{ref}) \tag{2}$$

Here e – electron charge,

ε_o – electrical constant,

c – speed of light,

$m*_n$ – effective mass of a free electron in GaN, defined through the mass of a free electron and equal to $m*_n = 0.19m_e$,

n_{ref} – refractive index;

and constant G_o for GaN takes a numerical value in the GHS system of units $6.07 \cdot 10^{-8}$.

Accordingly, the concentration of the donor impurity providing the required absorption coefficient should be equal to

$$N_d = \frac{1}{G_o}\frac{\mu_n}{\lambda^2} \cdot \alpha_n \tag{3},$$

and the conductivity of the GaN electrode layer can be represented as

$$\mu_n = G_o \cdot (\lambda^2 N_d)/\alpha_n \tag{4}$$

$$\sigma = en\mu_n = en \cdot G_o \cdot (\lambda^2 N_d)/\alpha_n \tag{5}$$

$$\rho = \frac{1}{en \cdot G_o}\frac{\alpha_n(\lambda)}{\lambda^2 \cdot N_d} \tag{6}$$

(taking into account that in the considered case GaN of n-type only is used, here and further we will assume that $\alpha_{GaN} = \alpha_n$)

The GaN/AlN/GaN epitaxial structure is one of the possible variants of the structure for a fully monocrystalline sensor, which we will consider as the initial one, and such a sensor can be characterized by its individual set of output parameters - thermal sensitivity *k*, response lag time *τ*, quality factor *k / τ,* etc.

For aluminum nitride AlN, which has a hexagonal lattice type, the polarization vector *P*, directed along the selected crystallographic direction (direction *c*), numerically coincides with the charge density *σ* on the opposite surfaces of the crystal normal to the axis *c* (their area *S* with layer thickness *w* and volume, respectively *V*). Then

$$P = \frac{1}{V}\sum_V q \cdot w = \frac{\Sigma q}{S} = \sigma \tag{7}$$

Polarization change ΔP in linear approximation is proportional to the temperature change, and the proportionality coefficient is defined as the pyrocoefficient χ, which is a material characteristic (as opposed to sensitivity k, which is proportional to the area of the active element of the sensor).

$$\Delta P = \chi \cdot \Delta T \tag{8}$$

$$\Delta(\Sigma q) = \chi \cdot S \cdot \Delta T = k \cdot \Delta T \tag{9}$$

The above expressions are usually applied to an ideal crystal, tacitly assuming homogeneity of the epitaxial layer along its thickness. However, the presence of intrinsic lattice defects (vacancies, inter-nodal atoms, clusters, etc.) have a noticeable effect on the

local values of the polarization vector, and the presence of mismatch dislocations of GaN and AlN lattice constants near their hetero-boundaries creates gradients of the pyrocoefficient values, which is experimentally observed when measuring the pyrocoefficient for different values of the AlN layer thickness. The character of this dependence has the form of a curve with saturation, which occurs at thicknesses of 100-120 mcm, and can be approximated by the following degree expression (on this subject, see Ref. [19]).

$$p(w) = p_0 \cdot \left(1 + \left(\frac{w}{w_0}\right)^2\right)^{-1} \tag{10}$$

The sensitivity of a pyroelectric sensor k is proportional to its active area S, which must be taken into account, taking into account the small area of light guides. Therefore, the question of possible ways to even slightly increase the sensitivity of such sensors seems to be relevant.

3 Modeling and computational details

The temperature change as a result of pulse heating of the pyrocrystal lattice is directly related to the amount of absorbed light energy; however, in the case of a complex layered structure characterized by inhomogeneous optical and thermophysical parameters, the absorption and heating processes acquire an extremely complex character.

It is well known from elementary optics that the absorption of light during its passage through a homogeneous medium on the optical path z in the linear case has an exponential character and is defined as follows: $B(z) = A_0 - A(z)$, where A_0 is incoming flow rate, $A(z)$ – its same value corresponding to its decrease with increasing z). Therefore, at passage of the impulse, the density of the absorbed energy has the form:

$$p(z) = dB(z)/dz \equiv A_0 \alpha_n \exp(-\alpha_n z) \tag{11}$$

If we assume adiabatic character of heat generation (and in most cases the pulse duration is τ<1ms, which is less than the characteristic times of heat redistribution), temperature profile $T(z)$ to a first approximation will retain its shape during the action of the beam (i.e., $T(t,z) = T(t) \cdot T(z)$), and at the end of the impulse it will qualitatively coincide with the distribution of the absorbed energy density $p(z)$. In the considered case, when optical and thermophysical parameters of each of the absorbing layers are assumed to be independent of coordinate and temperature, obtaining the distribution formed at the end of light exposure is reduced to solving the heat balance equation:

$$\Delta T(z) \cdot m \cdot C_V = A_0 \alpha_n \exp(-\alpha_n z) \quad \text{or}$$
$$\Delta T(z) = \left(\frac{A_0 \alpha_n}{m \cdot C_V}\right) \exp(-\alpha_n z) \tag{12}$$

where $\Delta T = T_{max} - T_0$ – temperature change during the pulse exposure,
C_V – specific heat capacity of the material,
m – mass of the object.

Based on (12), the temperature distribution within a single layer can be obtained; however, in a multilayer structure, each layer is characterized by its own set of parameters, which leads to non-uniform heat dissipation. Pulse heating of less transparent (GaN) layers can lead to a significant temperature increase; at the same time, heating of AlN layers or Al_2O_3 or SiC substrate at the end of the pulse will be practically absent. In addition, in the general case of multilayer structures, reflection effects from multiple hetero-boundaries can become significant, which is determined from the Fresnel formulas:

$$R_{1,2} = \frac{(n_2 - n_1)^2}{(n_2 + n_1)^2} \tag{13}$$

However, taking into account the closeness of the values of refraction coefficients of AlN and GaN (n_{GaN} =2.40, n_{AlN} =2.30), reflections from the boundaries and interference effects will be considered insignificant, and they will not be taken into account further. Therefore, without taking into account the superposition of direct and reflected waves, the modulus of the traveling wave will have the form:

$$A_1(z) = A_{01}\cdot\exp(-\alpha_1 z) \qquad z_1 \le z < z_2$$
$$A_{w1}(z = z_{12}) = A_{01}\cdot\exp(-\alpha_1 z_{12}) \qquad z = z_{12} = w_1 \qquad A_{01} = 1 \quad \text{(14a)}$$
$$A_2(z) = A_{02}\cdot\exp(-\alpha_2 z) \qquad z_2 \le z < z_3$$
$$A_{w2}(z = z_{23}) = A_{02}\cdot\exp(-\alpha_2 z_{23}) \qquad z = z_{23} = z_{12} + w_2 \qquad A_{02} = A_{d1} \quad \text{(14b)}$$

Due to the discrete one-dimensional nature of the layer structure of the sensor, the energy of the light flux completed on the path z $A(z)$, the absorbed light energy $B(z)$ and distribution of absorbed energy density $p(z)$ in a general form it is convenient to describe by a set of parameters $A_j(z)$, $B_j(z)$ and $p_j(z)$, each of them refers to a particular j-layer.

$$A_j(z) = A_{0j}\cdot\exp(-\alpha_j z) \qquad z_j \le z < z_{j+1}$$
$$A_{wj}(z = z_{j,j+1}) = A_{0j}\cdot\exp(-\alpha_j z_{j,j+1}) \qquad z = z_{j,j+1} = z_{j-1,j} + w_j$$
$$A_{0j} = A_{dj-1} \quad \text{(14c)}$$

Here j is a layer number, i defines the boundary number (including air boundaries), coordinates z_i are defined through the thickness of the i-th layer w_j as $z_{i+1} = z_i + w_j$, and in our particular case of the 7-layer system $j=1\div7$ and $i=1\div8$, A_j is an incoming luminous flux.

The values of absorption coefficients for 7 layers taking into account the substrate along the light flux can be represented as follows:

$$\alpha_j \in \left\{\alpha_{GaN1},\ \alpha_{AlN},\ \alpha_{GaN2},\ \alpha_{Ga_2O_3},\ \alpha_{GaN1},\ \alpha_{AlN},\ \alpha_{GaN2}\right\}$$

here $\alpha_{AlN} = 0$ and $\alpha_{Ga2O3} = 0$.

Using the condition of continuity of the light flux at the boundaries (see the conjugation condition 14c) we can construct a recurrence relation for calculating the full set of normalization constants A_{0j}

$$A_{i+1} = A_i\cdot\exp\left[-\left(\alpha_{j+1} - \alpha_j\right)z_{i+1}\right] \quad (15),$$

and the subsequent calculation of the total energy functions $A(z)$, $B(z)$ and $p(z)$ = grad $B(z)$.

Since the main technologically controllable parameters are layer thicknesses w_{GaN}, w_{AlN}, and α_{GaN} families of the indicated energy functions for different values w_{AlN} and w_{GaN} presented in Fig. 1 and families of the same functions for different values of the absorption coefficient α_{GaN}, presented in Fig. 2, were obtained. Applying the following procedure to calculate $p(z)$ to the ideology of equations (5)-(6) derivation, it is possible to obtain postimpulse temperature distributions $T(z)$, and from their averaged values within the layer $\langle T\rangle_j$.

To evaluate the efficiency of such a pyrometric sensor, it is advisable to introduce a criterion of the quality of its operation k_{pyr}, which would determine the configuration of its parameters in such a way as to ensure the maximum level of pyro-response at a given value of the amplitude of the output light flux and, taking into account the desirability of optimizing the cost of the epitaxial process, for some predetermined total thickness of epitaxial layers. Such a criterion can be defined as:

$$k_{pyr} = \chi\cdot A_7(z = z_8), \qquad w = Const \quad (16)$$

Obviously, such a criterion will reach its maximum value only at some optimal combination of sensor parameters. Fig. 3 shows a family of dependencies k_{pyr} of the layer thickness ratio for different values of the absorption coefficient, which demonstrates the technological possibilities of fine-tuning to ensure maximum pyroresponse values.
All calculations used in this work were performed in MATLAB software environment.

4 Conclusions

The observed trend of increasing role of minimally invasive and, in particular, subcutaneous operations suggests the development and introduction not only of new lasers and laser complexes, but also of means of diagnostics and control of energy parameters of pulsed laser radiation using new materials allowing *in vivo* operation. At the same time, the achieved level of development of epitaxial technologies of large-area nitrides already allows to create universal pyrometric sensors, compatible with elements of fiber optics and able to work from the mid-IR to near-UV range. Therefore, the search for ways to optimize the configuration of such AlN sensors, namely the calculation of the optimal ratio of the thickness of the active (AlN) and electrode (GaN) layers for different levels of light absorption and aimed at increasing their threshold sensitivity is relevant and timely.

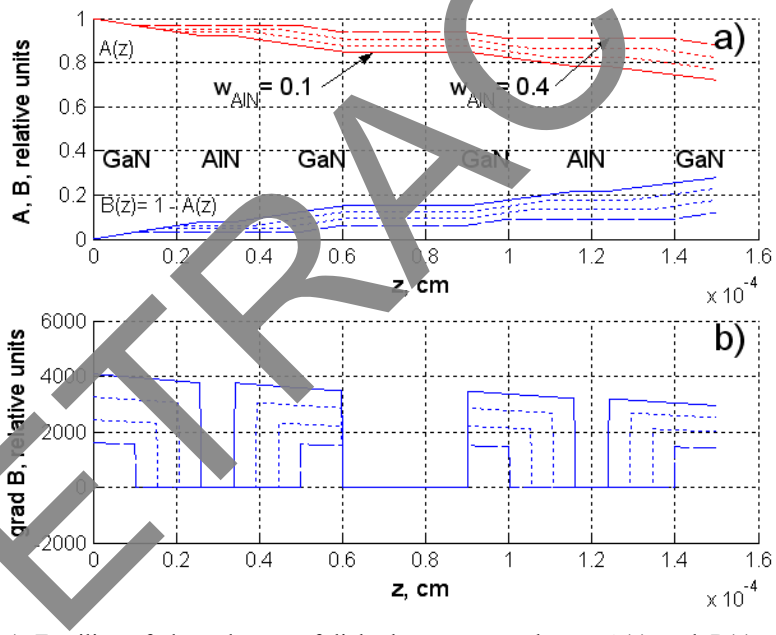

Fig. 1. a) Families of dependences of light beam energy losses A(z) and B(z) = 1- A(z) in GaN/AlN/GaN -- GaN/AlN/GaN multilayer structure for different thickness ratios w of AlN and GaN layers b) Postpulse distributions of absorbed energy density grad B(z) (temperature T) for different layer thickness ratios.

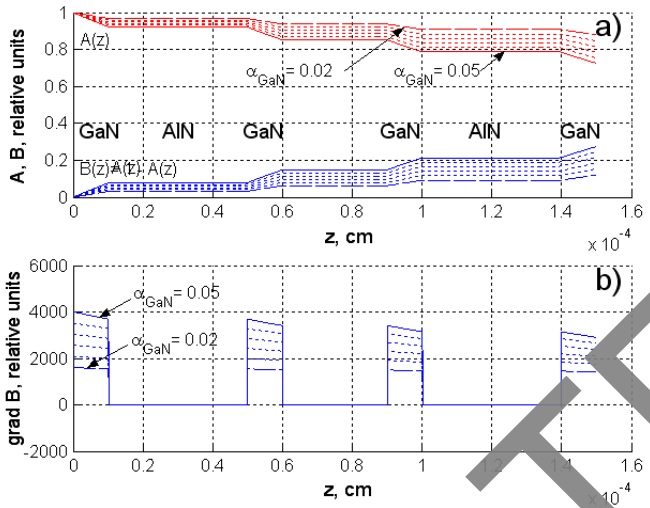

Fig. 2. (a) Families of dependences of light beam energy losses A(z) and B(z) in GaN/AlN/GaN -- GaN/AlN/GaN structure for different values of absorption coefficient α_{GaN}. (b) Postpulse distributions of the absorbed energy density grad B(z) (temperature T) for different values of the absorption coefficient α_{GaN}.

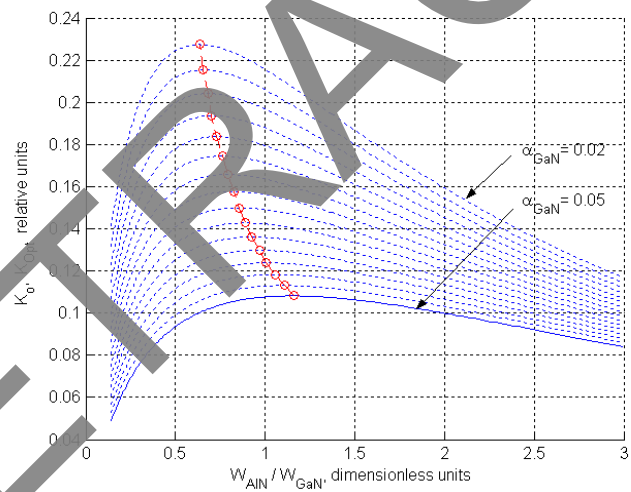

Fig. 3. Optimal values of ratios w_{AlN} / w_{GaN} providing maxima of the complex pyrocoefficient for different values of the absorption coefficient α_{GaN}.

References

1. M. Aleksandrova, C.Jagtap, V.Kadam, S.Jadkar, G.Kolev, K.Denishev and H.Pathan, Engineered Science, **16**, 82-89 (2021) DOI: 10.30919/es8d535
2. L. Lazov and T. Karadzhov, ETR, **3**,173-180 (2021) doi: 10.17770/etr2021vol3.6565.
3. E. Khalkhal, M.Rezaei-Tavirani, M.R.Zali, Z.Akbari. J. Lasers Med. Sci. **10** (suppl 1), S104-S111 (2019) doi: 10.15171/jlms.2019.S18

4. S.Bordignon, K.R.J.Chun, M.Gunawardene, B.Schulte-Hahn, B.Nowak, A.Fuernkranz et al. Expert Rev. Med. Devices. **10**, 2, 177-183 (2013) doi: 10.1586/erd.12.86.
5. S.V.Belov,Yu.K.Danileiko, A.B.Egorov, L.G.Shilin and A.M.Shulutko, Quantum Electron. **49,** 10, 982-987 (2019) doi: 10.1070/QEL16979
6. J.G.Miller, K.A.Horvath, Transmyocardial Laser Revascularization. In: Raja, S. (eds) Cardiac Surgery. Springer, Cham., pp 261–267 (2020) doi: https://doi.org/10.1007/978-3-030-24174-2_28
7. Z. Wang, M. Zhan, W. Li, C. Chu, D. Xing, S. Lu, X. Hu, A Journal of the German Chemical Society, **60**, 9, 4720-4731 (2021) doi:https://doi.org/10.1002/anie.202013301
8. P.Mroz, A.Yaroslavsky, G.B.Kharkwal, M.R.Hamblin. Cancers (Basel) **3**, 2, 2516-2539 (2011) doi: 10.3390/cancers3022516.
9. H.Abrahamse, M.R.Hamblin, Biochem. J., **473**, 4, 347-364 (2016) doi: 10.1042/BJ20150942.
10. N.M.Fried, Biomedical Optic Express, **9**, 9, 4552-4568 (2018) https://doi.org/10.1364/BOE.9.004552
11. K.E.Donaldson, R.Braga-Mele, F.Cabot, R.Davidson, D.K.Dhaliwal, R. Hamilton et al. J. Cataract Refract. Surg. **39**, 11, pp.1753-1763 (2013) doi: 10.1016/j.jcrs.2013.09.002.
12. C.B.Karuthedath, A.T.Sebastian, P.Helistö, T.Sillanpää, and A.Kärkkäinen, Journal of microelectromechanical systems, **32**, 5, 505-512 (2023) doi 10.1109/JMEMS.2023.3296159
13. C. Wang et al., Nature Biomed. Eng., **2**, 9, 687-695, (2018) doi: https://doi.org/10.1038/s41551-018-0287-x
14. B. Herrera, F. Pop, C. Cassella, M. Rinaldi, *"AlN PMUT-based ultrasonic power transfer links for implantable electronics"* in Proc. 20th Int. Conf. Solid-State Sensors, Actuators Microsyst. Eurosensors. Jun. 2019, pp.861-864 (2019) doi: 10.1109/TRANSDUCERS.2019.8808320
15. S.A.Kukushkin, S.S.Sharofidinov, Phys. Solid State, **61**, 12, 2342-2347 (2019) doi: https://doi.org/10.1134/S1063783419120254
16. E.A.Panyutin, S.S.Sharofidinov, T.A.Orlova, S.A.Snytkina, A.A.Lebedev, Tech. Phys., **65**, 3, 428-433 (2020) doi: http://dx.doi.org/10.1134/S1063784220030184
17. T.Kim, J.Kim, R.Dalmau, R.Schlesser, E.Preble, IEEE Transactions on Ultrasonics, Ferroelectrics, and Frequency Control, **62**, 10 1880-1887 (2015) doi: 10.1109/TUFFC.2015.007252
18. G.A.Gavrilov, A.F.Kapralov, K.L.Muratikov, E.A.Panyutin, A.V.Sotnikov, G.Y.Sotnikova, S.S.Sharofidinov, Tech. Phys. Lett., **44**, 8, 709-712 (2018) doi: http://dx.doi.org/10.1134/S1063785018080199
19. G.A.Gavrilov, K.L.Muratikov, E.A.Panyutin, G.Y.Sotnikova, S.S.Sharofidinov. Tech. Phys. Lett., **46**, 1, pp.16-18 (2020) doi: http://dx.doi.org/10.1134/S1063785020010058
20. M.A.Fraga, H.Furlan, R.S.Pessoa, M.Massi, Microsyst. Technol., **20**, 9-21 (2014) doi: https://doi.org/10.1007/s00542-013-2029-z
21. E.A.Panyutin, M.L.Shmatov, Quantum Electron., **49**, 11, 1078-1082 (2019) doi: http://dx.doi.org/10.1070/QEL16917